

Continuous and simultaneous measurement of triple oxygen and hydrogen isotopes of liquid and vapour during evaporation

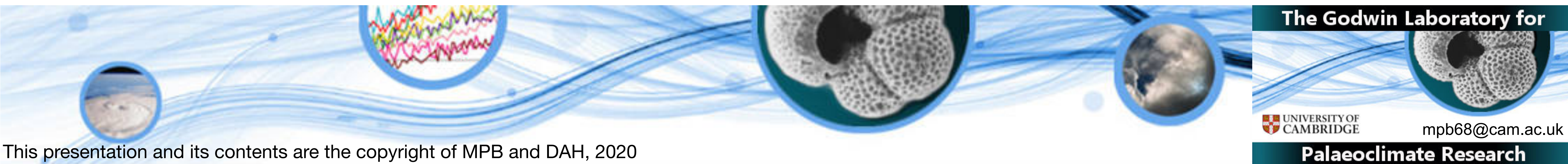
Matthew P. Brady & David A. Hodell

Godwin Lab, Dept. Earth Sciences, Downing Street, Cambridge CB2 3EQ

AIM: Conduct evaporation experiments under a variety of conditions with semi-continuous and simultaneous measurements of triple oxygen and hydrogen isotopes at high precision. Explore precision of derived parameters $^{17}\text{O}_{\text{xs}} (= \ln(\delta^{17}\text{O}/1000+1) - 0.528 \cdot \ln(\delta^{18}\text{O}/1000+1))$ and $D_{\text{xs}} (= \delta\text{D} - 8 \cdot \delta^{18}\text{O})$ that can be obtained using long injections of water to the Picarro instrument using a non-standard technique.

METHODS: Built an integrated experimental and measurement system comprising a COY evaporation chamber, Ismatec peristaltic pump, and Picarro L2140-*i* cavity ring-down spectroscopy instrument with Picarro Standards Delivery Module (SDM).

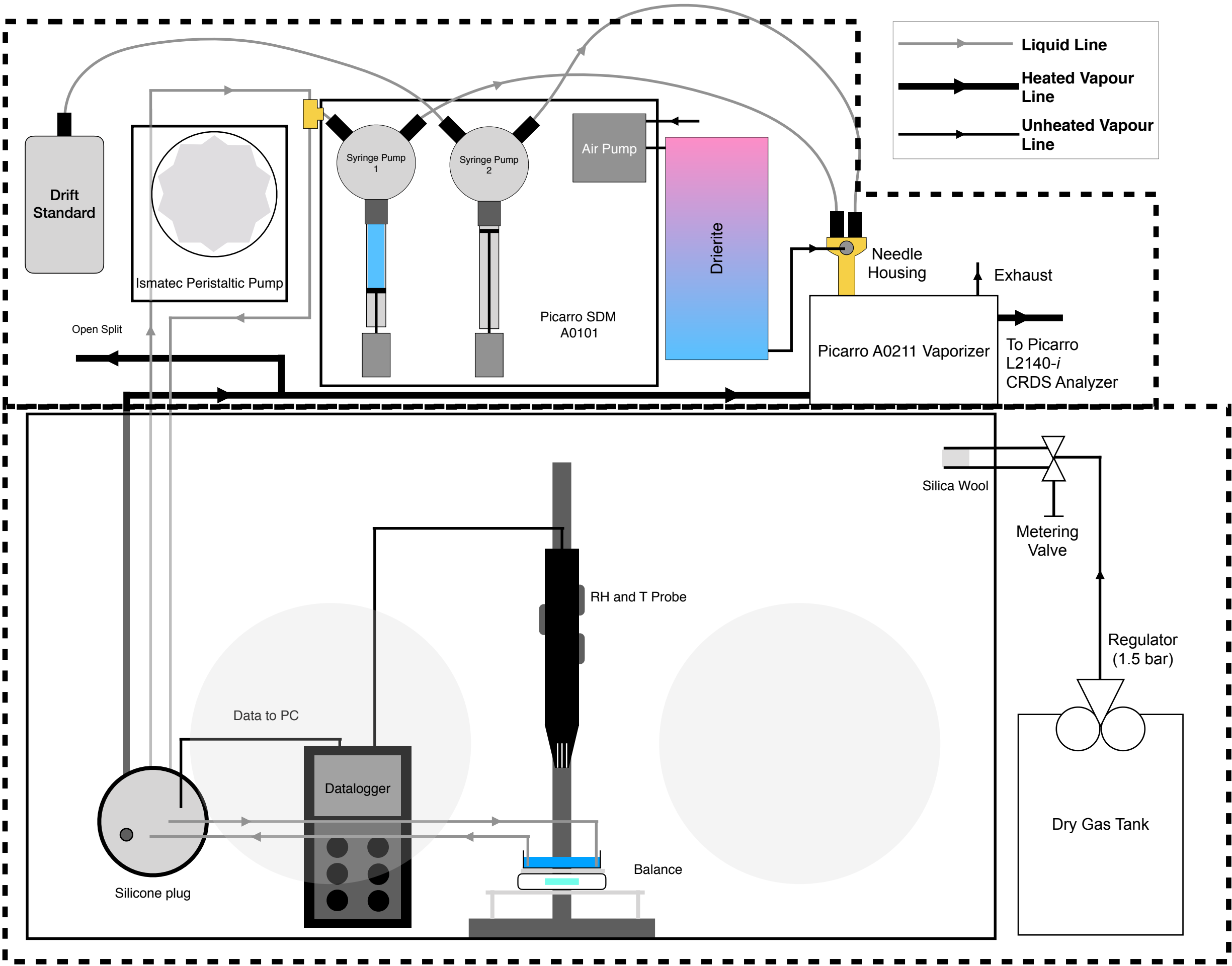
RESULTS: Across a single 40-minute injection, we achieve standard error precision of 0.008 ‰ for $\delta^{17}\text{O}$ and $\delta^{18}\text{O}$, 6 per meg for $^{17}\text{O}_{\text{xs}}$, 0.02 ‰ for δD , 0.08 ‰ for D_{xs} . For a 12-minute vapour measurement, we achieve standard error precision of 0.013 ‰ for $\delta^{17}\text{O}$, 0.011 ‰ $\delta^{18}\text{O}$, 9 per meg for $^{17}\text{O}_{\text{xs}}$, 0.02 ‰ for δD , 0.1 ‰ for D_{xs} . These high precisions, combined with large number of data points per experiment result maximum 95% confidence interval on the slopes for $\ln(\delta^{17}\text{O}+1)$ vs $\ln(\delta^{18}\text{O}+1)$ of ± 0.0004 and ± 0.0006 for the liquid and vapour, respectively. For the slopes of $\ln(\delta\text{D}+1)$ vs $\ln(\delta^{18}\text{O}+1)$ we calculate maximum 95% confidence intervals of ± 0.03 for the liquid and vapour phases, however, there is clear curvature to these trends additional processes may be acting on the system. The calculation of α_{evap} from our experiments highlights a small offset between the liquid and vapour phases for all isotopes. For oxygen isotopologues, the trend follows the predicted values, but with an offset. For Hydrogen isotopes, the relationship between the predicted α_{evap} and the measured is more complex.



Experimental Set Up - Schematic

Measurement system

Picarro L2140-*i* cavity ring-down spectroscopy (CRDS) instrument with Picarro Standards Delivery Module (A0101), and Ismatec IPC Peristaltic Pump



Experimental system

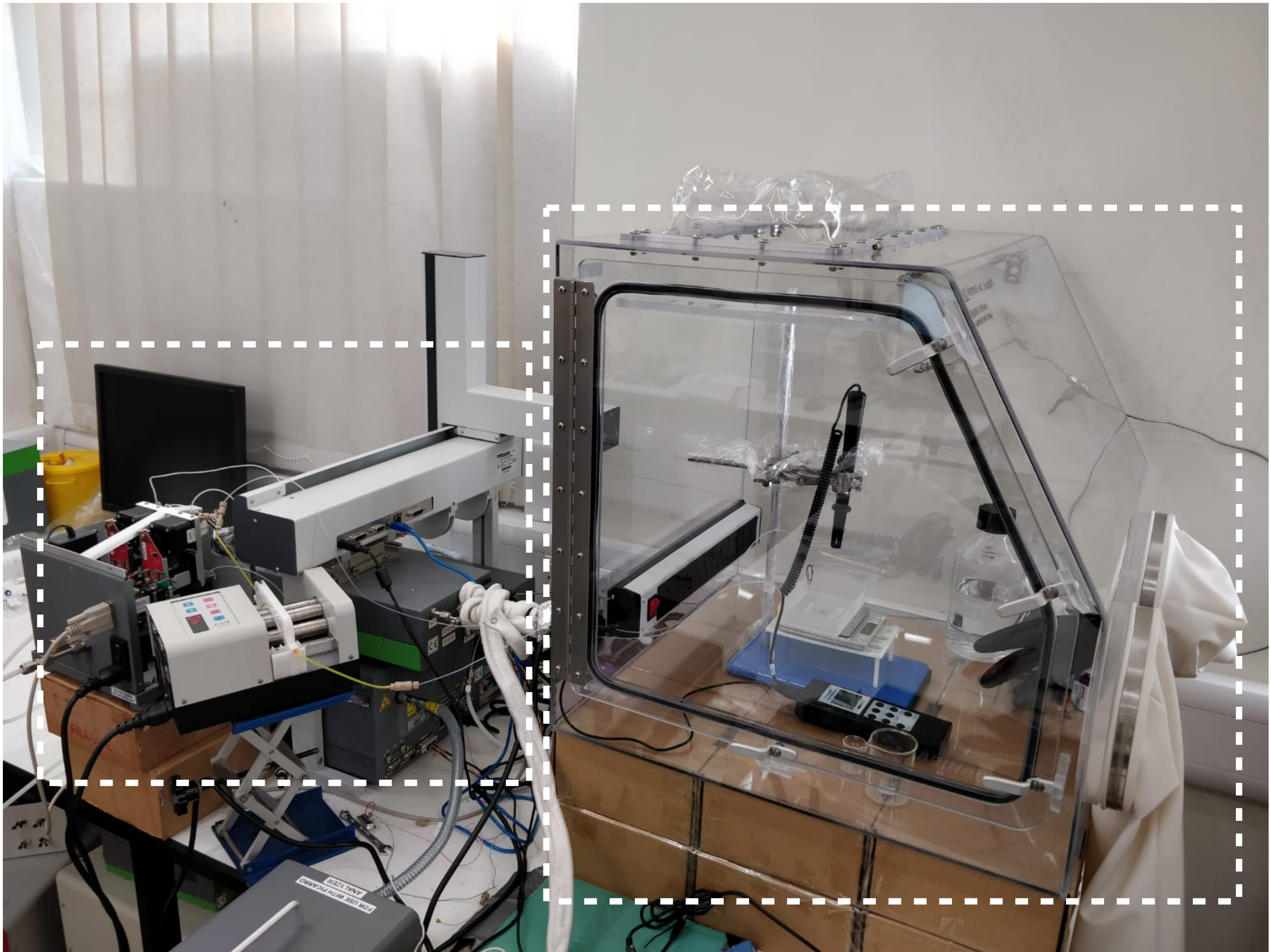
0.4 m³ Coy Labs glovebox (8302050)

Figure 1a - Two part set up, divided into measurement and experiment halves

Experimental Set Up

Measurement system

Picarro L2140-*i* cavity ring-down spectroscopy (CRDS) instrument with Picarro Standards Delivery Module (A0101), and Ismatec IPC Peristaltic Pump

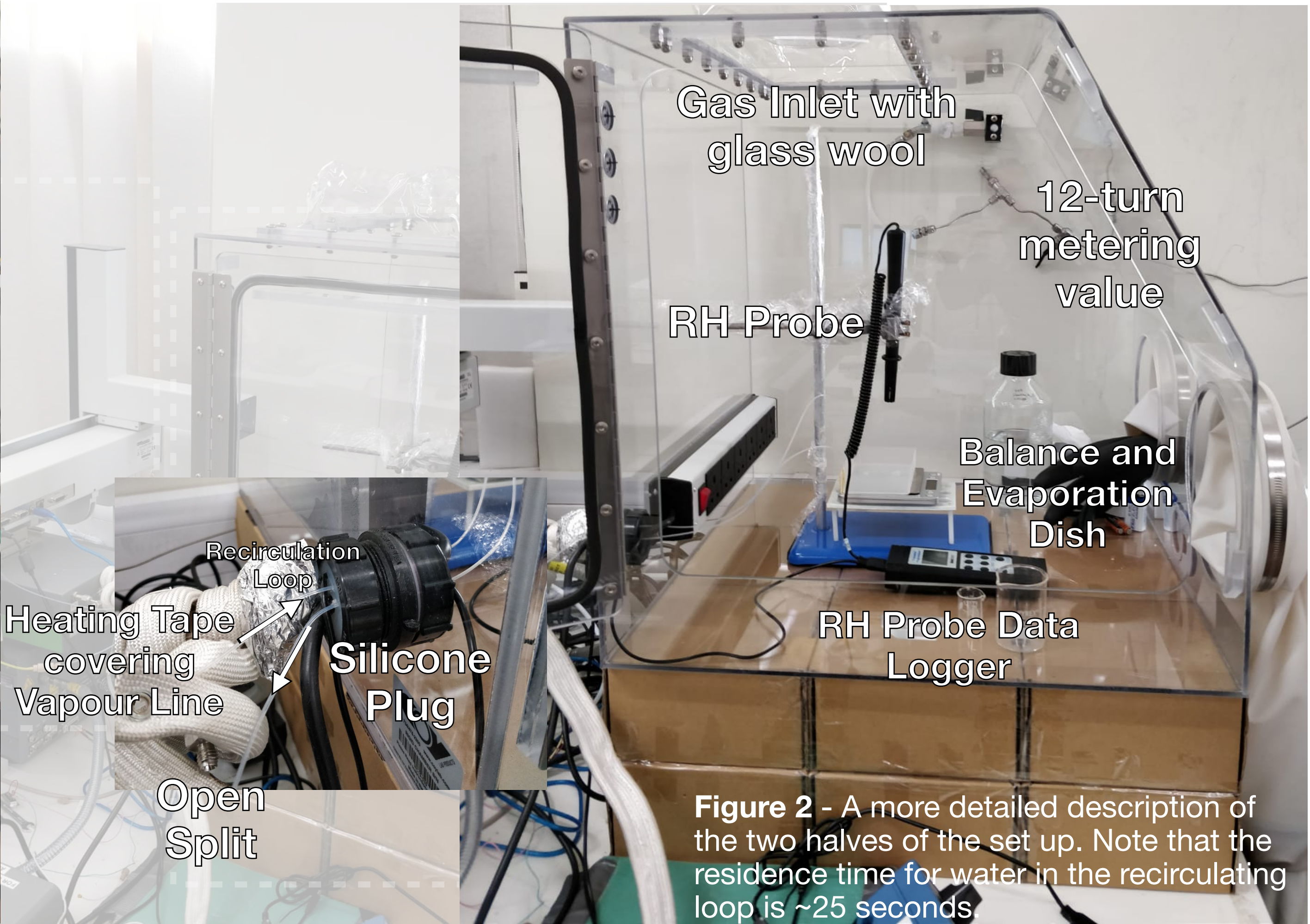


Experimental system

0.4 m³ Coy Labs glovebox (8302050)

Figure 1b - Two part set up, divided into measurement and experiment halves

Experimental Set Up



Allan Variance Analysis

To optimise liquid injection length, we conduct Allan variance analysis by resampling a large, isotopically homogenous, sealed volume of deionised water^{1,2}.

Water was recirculated using the peristaltic pump and sampled by the SDM every 30-minutes over the course of ~42-hours. Target H₂O was 20,000 ppmV

Used built-in `allanvar` MATLAB function to calculate where deviation due to instrument noise is minimised.

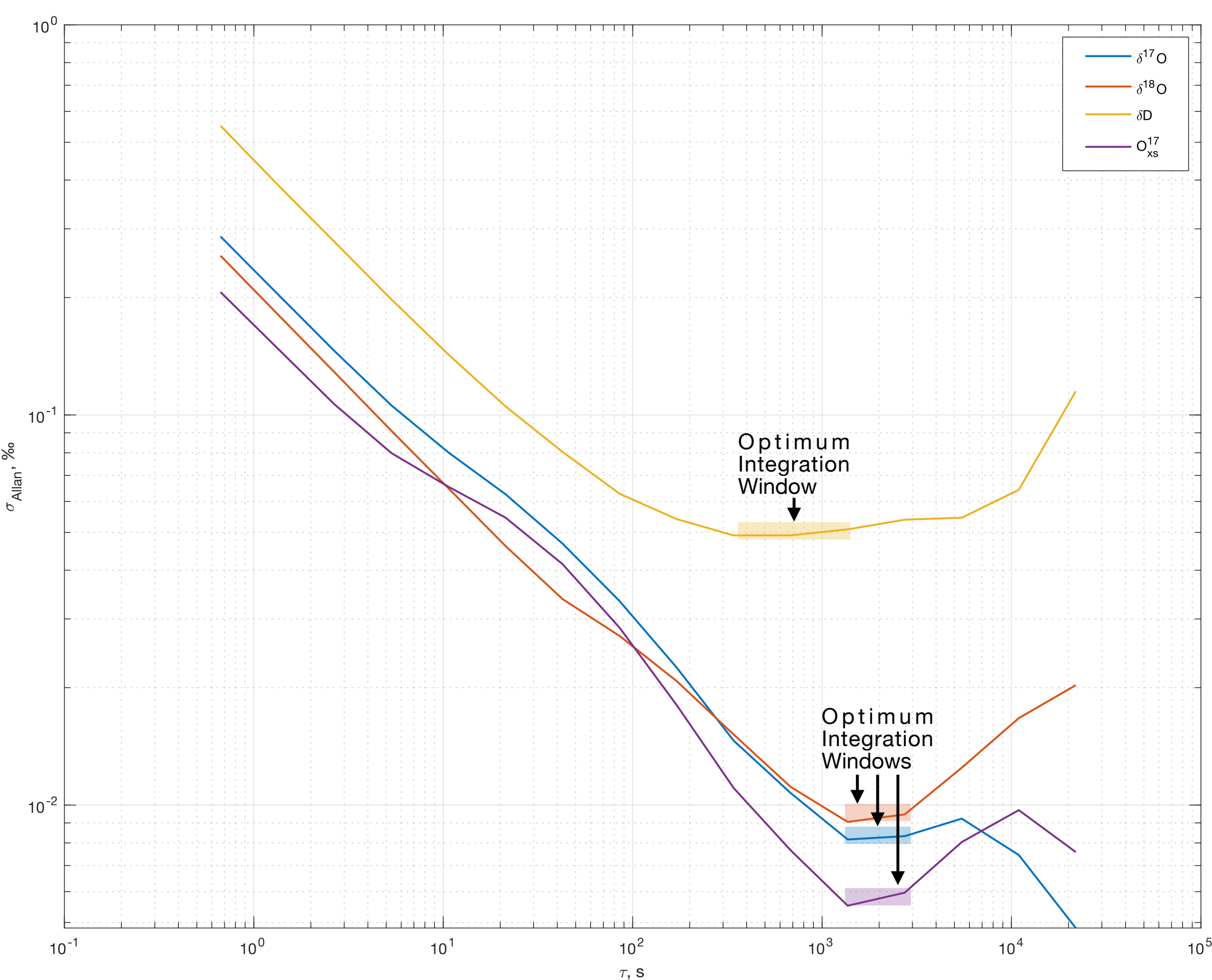


Figure 3 - The Allan variance as determined by the built-in MATLAB `allanvar` functionality. For $\delta^{17}\text{O}$ and $\delta^{18}\text{O}$, Allan variance decreases linearly until it reaches the noise floor window, $\tau \sim 1350\text{--}2760$ seconds (highlighted). This period is the same for $^{17}\text{O}_{\text{xs}}$. For δD , the noise floor window is shorter than for oxygen isotopologues, $\tau \sim 340\text{--}1400$ seconds (highlighted). Beyond these highlighted windows, instrument drift becomes incorporated into the integrated signal and precision worsens as a result.

¹Allan (1966); ²Gkinis *et al.* (2010)

Experimental Sequence

Based on Allan variance analysis, we use the *SDM Pump Sequencer* to define a measurement sequence which incorporates a light standard (*JRW*) and a heavy standard (*MPB Enr*) followed by a drift check standard (*MPB Tap*) each for 40-minutes at two H₂O concentrations (20,000 ppmV and 12,500 ppmV).

Measurement alternates between sampling Experimental Vapour (from Evaporation Chamber) and Experimental Liquid (sourced from the SDM) on an 88-minute cycle.

Drift standard is re-measured every ~14h and standards are re-run at experiment termination.

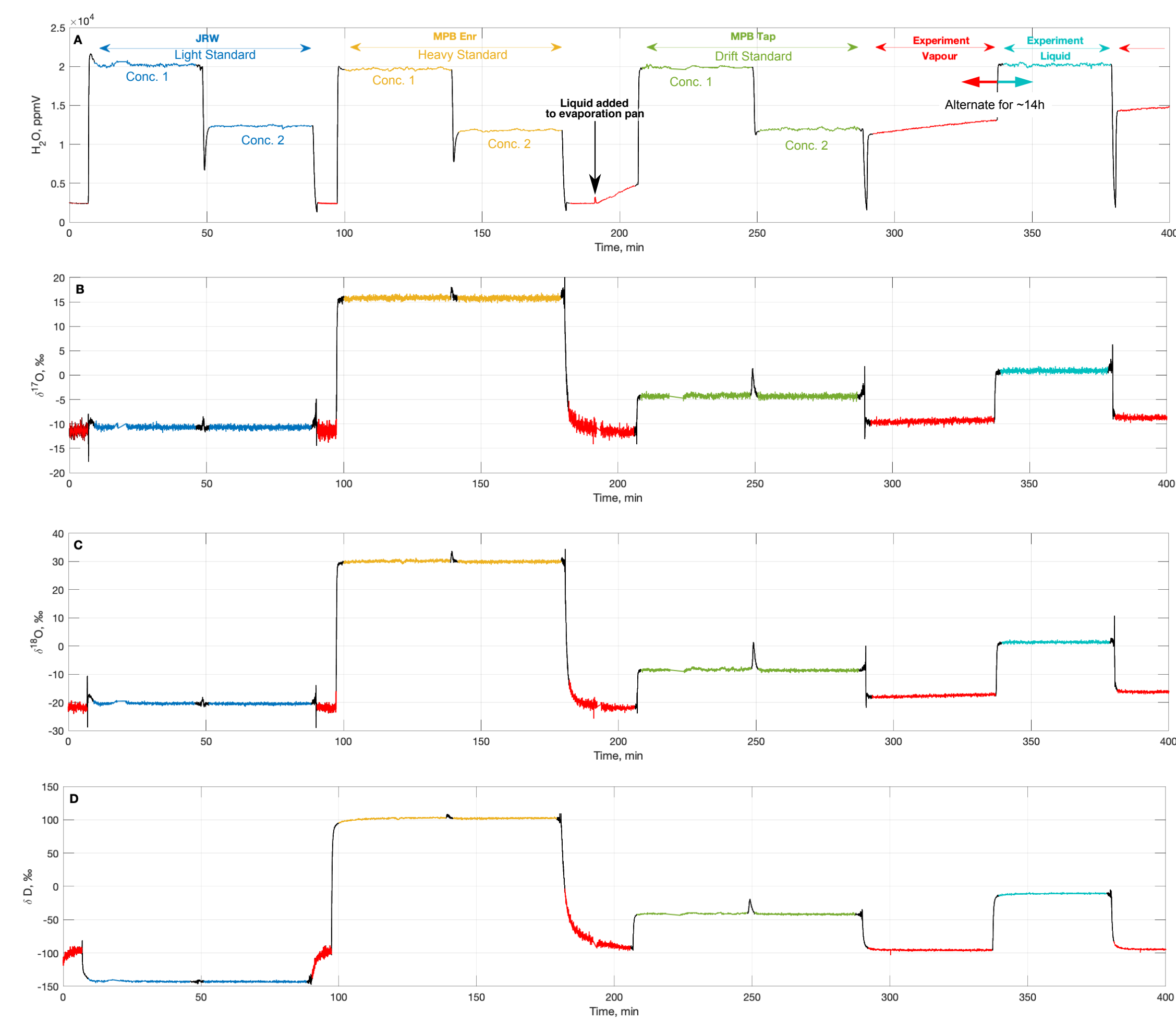


Figure 4 - These panels show what is recorded by the Picarro L2140-*i* analyzer at the start of an evaporation experiment. Coloured windows represent a different material being introduced to the analyzer. First, the two VSMOW-SLAP calibrated in-house standards, then the drift standard, followed by alternating Experimental Vapour and Experimental Liquid.

Memory, Response Time, and Precision - Liquid Injections

Memory is greatest at the beginning of a liquid injection where a small amount remains from a previous sample, upstream of the vaporizer.

To reduce this volume, we manually shortened the teflon tubing from *Syringe Pump 1* to the needle housing to 15 cm.

At target SDM pump rate, 0.05 $\mu\text{L s}^{-1}$, this takes four-minutes to clear.

To ensure memory effects are accounted for, we remove an additional two-minutes of data for oxygen isotopologues and 13-minutes of data for hydrogen (to take advantage of Allan variance minimum).

Table 2 - The average standard deviation and standard error of all liquid injections during a typical experiment. All data points for an injection, after memory windows are applied, are included. Number of injections=72. Data points for each injection ~1370 for oxygen isotopologues and ~925 for deuterium. *per meg

Isotope	Data window length, minutes	Average SD, ‰	Average SE, ‰
$\delta^{17}\text{O}$	34	0.28	0.0081
$\delta^{18}\text{O}$	34	0.25	0.0076
δD	23	0.60	0.020
$\text{O}^{17}_{\text{xs}}$	34	210*	5.8*
D_{xs}	23	2.4	0.080

Memory, Response Time, and Precision - Vapour measurements

Using an adapted Heavside function we calculate the response of the cavity as it changes from liquid to vapour measurements and remove this from the beginning of each 40-minute vapour measurement period³.

At extreme evaporation, internal gradient of each 40-minute measurement period increases as rate of change of measured isotope increases.

Therefore, we divide each vapour measurement to three 750 second measurements. This minimises both internal gradient and maximises precision.

Table 3 - The average measurement gradient, standard deviation, and standard error of all liquid injections during a typical experiment. Each vapour period split into 750 second windows containing ~500 data points. Number of measurements=216. *per meg min⁻¹ ** per meg

Isotope	Measurement gradient, ‰ min ⁻¹	Average SD, ‰	Average SE, ‰
δ ¹⁷ O	1.9 x 10 ⁻⁴	0.28	0.013
δ ¹⁸ O	2.3 x 10 ⁻⁵	0.25	0.011
δD	-0.014	0.52	0.023
O ¹⁷ _{xs}	0.17 *	210 **	9.2 **
D _{xs}	-0.014	2.2	0.099

³Jones *et al.* (2017)

Evaporation Experiments - Evaporative Trends

The deuterium data in both the liquid and the vapour phase closely follow expected trends with respect to RH. However, there is curvature apparent in the δD vs $\delta^{18}O$ (**4A** and **4B**) relationships and in the D_{xs} vs $\delta^{18}O$ (**4C** and **D**) relationships which require further investigation.

The relationship between the oxygen isotopologue fractionation factors is given by the equation⁴:

$$\lambda = \frac{{}^{17}\alpha_{evap} - 1}{{}^{18}\alpha_{evap} - 1}$$

(Eq.1)

This lambda is also the same as the regression for the slope $\ln(\delta^{17}O+1)$ vs $\ln(\delta^{18}O+1)$ ⁴, and therefore can be precisely calculated from our data.

Table 4 - Regression slopes for $\ln(\delta^{17}O+1)$ vs $\ln(\delta^{18}O+1)$, here reported as λ of either the liquid phase or the vapour phase. All $R^2=1.0000$ with residuals $<0.05 \times 10^{-3} \text{ ‰}$.

RH, % (1sd)	Liquid data points	λ_{liq} , (2sd)	Vapour data points	λ_{vap} , (2sd)
23.2 (0.3)	53	0.5254 (0.0003)	158	0.5299 (0.0006)
36.4 (1.5)	71	0.5249 (0.0003)	230	0.5266 (0.0004)
53.9 (1.7)	88	0.5239 (0.0003)	237	0.5226 (0.0002)
74.9 (1.4)	66	0.5212 (0.0004)	259	0.5222 (0.0003)

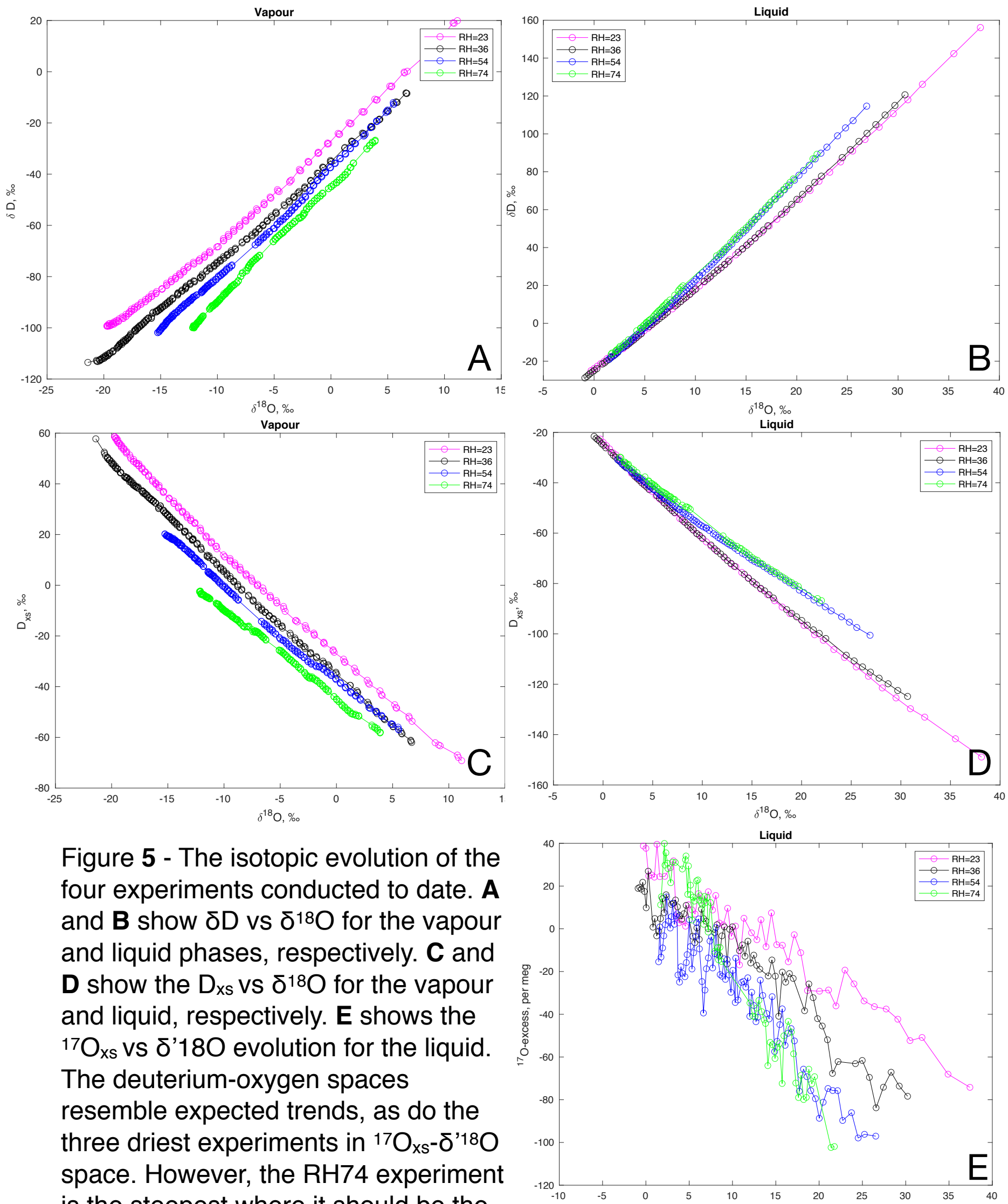


Figure 5 - The isotopic evolution of the four experiments conducted to date. **A** and **B** show δD vs $\delta^{18}O$ for the vapour and liquid phases, respectively. **C** and **D** show the D_{xs} vs $\delta^{18}O$ for the vapour and liquid, respectively. **E** shows the $^{17}O_{xs}$ vs $\delta^{18}O$ evolution for the liquid. The deuterium-oxygen spaces resemble expected trends, as do the three driest experiments in $^{17}O_{xs}$ - $\delta^{18}O$ space. However, the RH74 experiment is the steepest where it should be the shallowest.

⁴Barkan and Luz (2007)



Evaporation Experiments - Alpha Calculations

We conducted four experiments at different relative humidities by changing the flow of dry gas through the box. The only source of water vapour in the box is the evaporating fluid, therefore the isotopic evolution of the remaining fluid is controlled by the Rayleigh fractionation equation⁵:

$$*R = *R_o \times f^{(1/*\alpha_{evap}-1)} \tag{Eq.2}$$

*R is the isotope ratio of interest, f is the mass fraction of liquid remaining, and *α_{evap} is the evaporative fractionation factor (combining kinetic and diffusional processes). The expected value for *α_{evap} under these conditions is given by the equation⁴:

$$*\alpha_{evap} = *a_{eq}(*a_{diff}(1 - RH) + RH) \tag{Eq. 3}$$

Where *α_{eq} is the temperature dependent equilibrium fractionation factor, and *α_{diff} is the turbulence dependent diffusional fractionation factor.

We calculate *α_{evap} for our experiments by plotting ln(1000+δ*) vs ln(F) for each RH. Our large datasets for liquid and vapour allow calculation of the fractionation factor to 95% confidence of 0.0001, 0.0002, and 0.002 for ¹⁷α_{evap}, ¹⁸α_{evap}, and ²α_{evap}, respectively. However, we observe constant offset between liquid and vapour alphas at different RH, and between *α_{evap} predicted by Eq. 3.

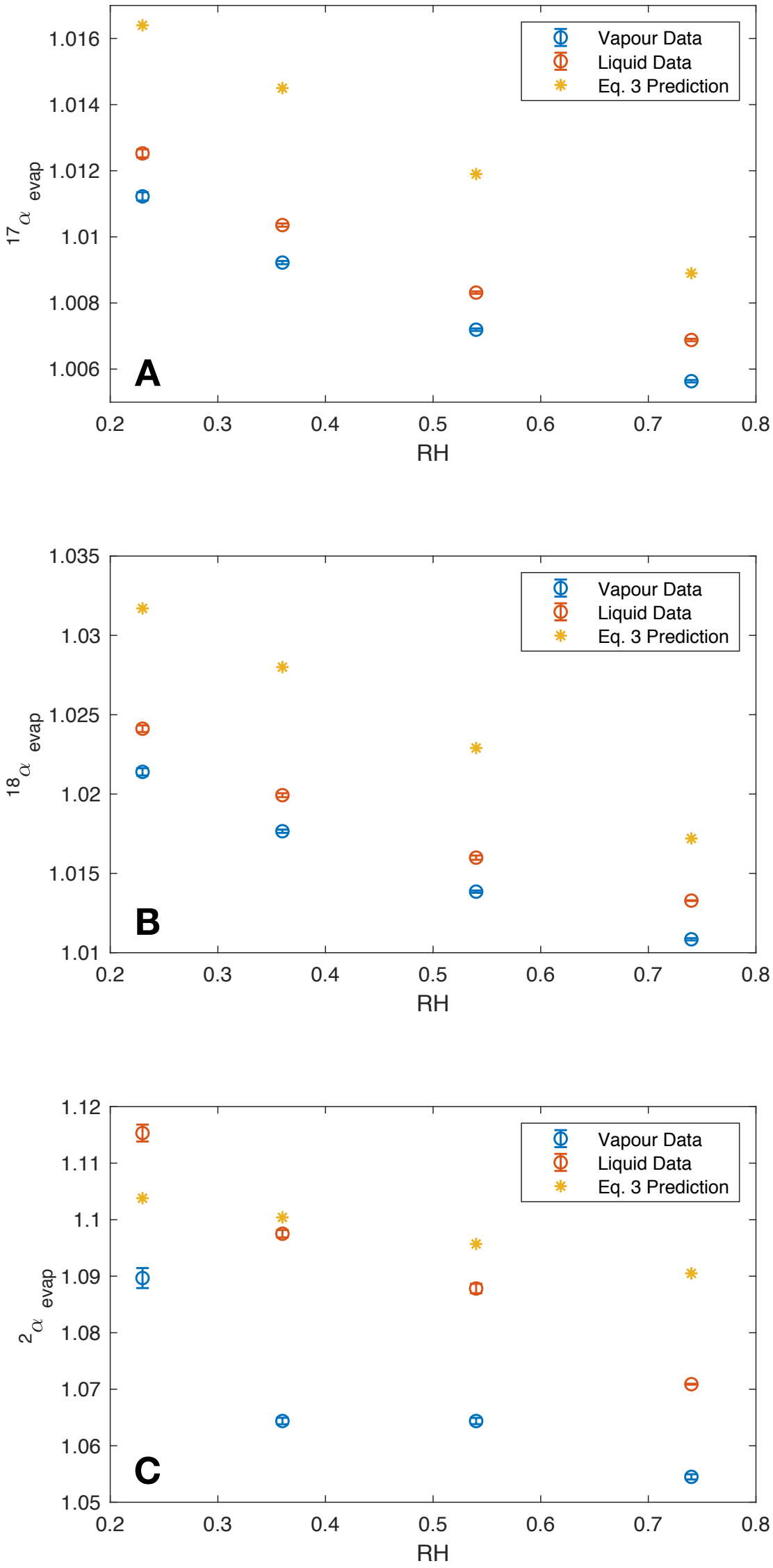
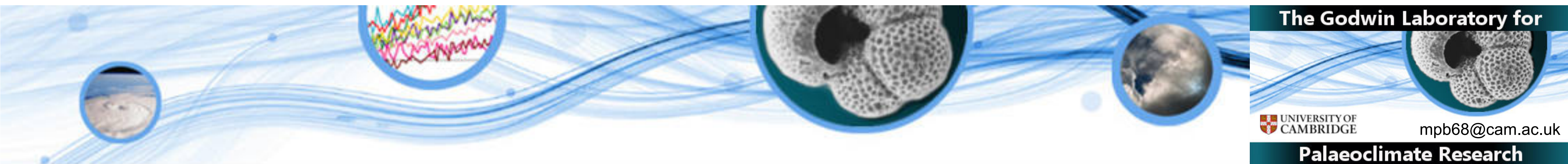


Figure 6 - All panels show how the fractionation factors for liquid and vapour of water isotopes change under different RH conditions. The oxygen isotopologues (panels **A** and **B**) display a constant offset between the liquid and vapour under all RH conditions, with the offset between the model value and measured values decreasing slightly with decreasing RH. Panel **C** shows the deuterium fractionation factors which display a more complex relationships between liquid and vapour as well as between the calculated values and the model predictions. In this figure, we use a pure diffusional term when calculating *α_{diff} for later use in Eq. 3.

⁵Criss (1999); ⁴Barkan and Luz (2007)

Conclusions

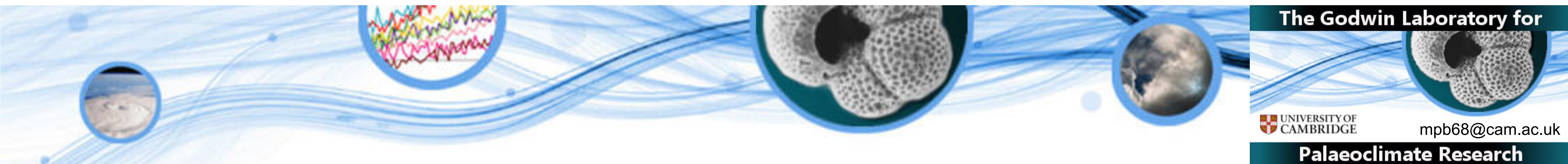
- Highly precise measurements of triple-oxygen and hydrogen isotopes can be made simultaneously and continuously for the liquid and incident vapour of an evaporating water body.
- This is achieved by combining existing Picarro hardware (Standards Delivery Module) and an Ismatec Peristaltic Pump with a sealed, highly controllable Coy Labs glovebox (which acts as an evaporation chamber).
- After processing, the 95% confidence window on the $\ln(\delta^{17}\text{O}+1)$ vs $\ln(\delta^{18}\text{O}+1)$ is ± 0.0004 and ± 0.0006 for the liquid and vapour, respectively. For the slopes of $\ln(\delta\text{D}+1)$ vs $\ln(\delta^{18}\text{O}+1)$ we calculate maximum 95% confidence intervals of ± 0.03 for the liquid and vapour phases, but there is some curvature to these slopes which requires further investigation.
- Fractionation factors $^{17,18}\alpha_{\text{evap}}$ predicted values, but with a constant offset. The $^{\text{D}}\alpha_{\text{evap}}$ is more complex.



Future Work

- Conduct experiments which better explore the experimental space. For example, that are conducted in an already humid atmosphere, or at different temperatures, or which explore transient changes in RH and the effect on isotope evolution
- Conduct Montecarlo simulations of evaporation to fully constrain evaporation chamber conditions
- Explore the relationship between surface area and volume on isotope evolution using 3D printed idealised basins
- Examine a real-world closed-basin isotopic evolution by using 3D printed lake bathymetry and compare results to gypsum hydration water data
- Expand the experimental set up to examine other hydrological systems, such as caves or playas

Many thanks to...



References

- 1 Allan DW. Statistics of atomic frequency standards. *P IEEE*. 1966;54(2):221-230. doi:10.1109/proc.1966.4634
- 2 Gkinis V, Popp TJ, Johnsen SJ, Blunier T. A continuous stream flash evaporator for the calibration of an IR cavity ring-down spectrometer for the isotopic analysis of water. *Isot Environ Healt S*. 2010;46(4):463-475. doi:10.1080/10256016.2010.538052
- 3 Jones TR, White JWC, Steig EJ, et al. Improved methodologies for continuous-flow analysis of stable water isotopes in ice cores. *Atmos Meas Tech*. 2017;10(2):617-632. doi:10.5194/amt-10-617-2017
- 4 Criss, R.E., 1999. Principles of stable isotope distribution. Oxford University Press on Demand.
- 5 Barkan E, Luz B. Diffusivity fractionations of $\text{H}_2^{16}\text{O}/\text{H}_2^{17}\text{O}$ and $\text{H}_2^{16}\text{O}/\text{H}_2^{18}\text{O}$ in air and their implications for isotope hydrology. *Rapid Communications in Mass Spectrometry*. 2007;21(18):2999-3005. doi:10.1002/rcm.3180

